Proceedings of the South Baltic Conference on
Dredged Materials in Dike Construction
Rostock, 10-12 April 2014
ISBN: 978-3-86009-409-9
www.dredgdikes.eu

DEFORMATION ANALYSIS OF DIKES USING UNMANNED AERIAL SYSTEMS (UAS)

Matthias Naumann[1], Ralf Bill[2], Frank Niemeyer[3], Elisabeth Nitschke[4]

[1,2,3] Chair for Geodesy and Geoinformatics, Rostock University,18059 Rostock, German,, [matthias.naumann] [frank.niemeyer] [ralf.bill] @uni-rostock.de
[4] Chair of Geotechnics and Coastal Engineering, Rostock University,18059 Rostock, Germany, elisabeth.nitschke@uni-rostock.de

Abstract. The main focus of the paper is a comparative study, in which we have investigated, whether automatically generated digital surface models (DSM) obtained from unmanned aerial systems (UAS) imagery are suitable for the detection of deformations or shape changes over time of dike constructions or similar structures. This research is conducted at a test dike located in Rostock, Markgrafenheide (Germany) and its surrounding site. The test dike of 130 m in length, up to 48 m in width and 3.3 m in height consists of three polders and serves in long-term studies for testing the suitability of dredged material in dike construction. For the comprehensive investigation of processes such as subsidence, consolidation and increased surface erosion, the comparisons of high-resolution DSMs of different times (change detection) are appropriate. Instead evaluations at a few points, as in conventional surveying method, much more detailed analyzes are now possible, based on the comparison of dense surface models. UAS (also called Unmanned aerial vehicles (UAV) or Remotely piloted aircraft systems (RPAS)) have become a rapidly growing research topic for photogrammetry and geoinformatics. Electric motor-driven lightweight Micro-UAS have proved to be flexible acquisition systems for the generation of high-resolution DSMs and ortho photo image mosaics of smaller areas. Compared to conventional surveying methods, e.g. Terrestrial Laser Scanners (TLS) and tacheometry UAS photogrammetry is a very fast and cost-effective 3D-surveying method. In our research aerial images were acquired by a nadir-looking camera transported and controlled by Micro-UAS in multicopter-design. Two different systems were used: First, the MD4-1000 from Microdrones with a digital camera PEN e-P2 from Olympus and a fixed focal length lens of 17 mm and secondly, the AscTec Falcon 8 from Ascending Technologies with the NEX-5 from Sony and focal length lens of 16 mm. The area of study was surveyed six times: twice during the constructions and four times after completion. Our deformation analyzes are based on the four epochs after completion (June 2012 to June 2013). For the automatically processing of the imagery state-of-the-art processing service PIX4UAV Cloud by PIX4D were used to compute the photogrammetric products (PIX4D, 2014). The spatial resolution of the derived DSM is between 0.013 to 0.026 m. The verification of the DSM showed standard deviations of the height differences between 2 and 3 cm. By difference calculations based on the zero epoch, the expected changes in the surface levels could be detected. For comparable terrain surfaces height changes can be very effectively monitored, if their magnitudes are above the measurement uncertainty and the change of vegetation heights between epochs.

Keywords: Change Detection, Subsidence, DSM, UAS, 3D point cloud, accuracy

1. Motivation

Detailed statements on structures and buildings with respect to their long-term behavior can be derived based on large scale multi-year experiments. The so-called Rostocker testdike, constructed as part of the EU-funded project "Project DredgDikes", serves for investigations into the suitability of dredged materials for future dike construction works. A major complex of investigations thereby represents the structural monitoring, which determined and documented the geometric changes of the construction in its position, shape and size caused by processes e.g. reductions and shrinkage.

For reasons of economy, the deformations were often observed only at selected points, which represent the expected changes appropriate. Their positions were determined with conventional measuring techniques such as tacheometry or close-range photogrammetry. In contrast, the surface-based analysis of deformations was

Selection and peer-review under responsibility of Universität Rostock / scientific committee of the conference

uneconomical in most applications, due to the time consumed of the measurements or the evaluations.

In recent years, the automation of the technologies and the processing reached a level that enables efficient surface-based measurement method of high spatial resolution. The rapidly developed UAV photogrammetry (Eisenbeiss, 2009), which is characterized by comparatively very fast data acquisition during a flight over by an UAS and largely autonomous evaluation processes is now pushing into the applications of the TLS and of the close-range photogrammetry. Various photogrammetric output products, in addition to the ortho photo mosaic, a point cloud and the DSM are results of the automatic processing pipeline, which starts from the aerial image sequences of the object of interest.

In addition, the UAS images or the ortho photo mosaic included as an advantage over the TLS, the texture information of the surface, which has a documentary value and is, for example, suitable for the analysis of the vegetation state or image-visible erosions.

Today, a plurality of electrically driven autonomous flight systems in multicopter-design (Micro-UAS) with load capacities of up to 1.5 kg are commercially available and the legal regulations for their application are relatively easy to meet. The suitability for use of these Micro-UAS for 3D surface reconstruction of terrains up to several hectares has been demonstrated in recent years in a variety of scientific studies (e.g. Eltner et al., 2013; González-Aguilera et al., 2012; Sauerbier et al., 2011; Eisenbeiss and Zhang, 2006).

The time savings of UAS photogrammetry compared with the also largely automated measurement method TLS is very high. This is achieved by very short on-site measurement duration. In a comparison of both methods using the example of the test dike, the UAS photogrammetry required only about 50% of the time of the TLS. With the increasing complexity and also the extent of the object even more saving effects can be expected (Naumann et al., 2013).

Eltner et al., 2013 investigated the accuracy of such UAS DSM and their combination with TLS for the quantitative measurement of soil erosion. Thereby they compared different software solutions for the UAS image processing. González-Aguilera et al., 2012 analysed the accuracy of a UAS DSM with a simultaneously recorded TLS DSM using the example of granite mine.

In this study, we used the Microdrones MD4-1000 and the Falcon 8 as UAS in combination with the web processing service Pix4UAV, which offers fully automated DSM generation (Pix4D, 2014). This means that for constructions on the order of the test dike with its complex structure - various cross sections, internal polders and changing combinations of materials - now not only studies at some points, but rather much more detailed analysis, based on comparing surfaces of multiple epochs are possible (multi-temporal change detection).

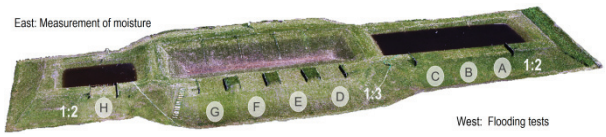

Fig 1. Photorealistic textured DSM of the Rostock test dike (University of Rostock, Naumann and Cantré)

2. Area of study

This research is conducted at a test dike located in Rostock, Markgrafenheide (Germany) and its surrounding site, which together cover an area of about 3 hectares. The size and extent of the test dike is well suited for the use of small UAS with little payload capacities (Naumann et al., 2013).

The large-scale experimental dike work was built as part of the international and EU part-financed project DredgDikes (http://www.dredgdikes.eu/) which is coordinated by the Chair of Geotechnics and Coastal Engineering at the University of Rostock. It serves in long-term studies for testing the suitability of dredged material in dike construction to replace the commonly used materials, marl and clay, which were becoming increasingly scarce in recent years (Cantré and Saathoff, 2013).

The test dike of about 130 m in length, up to 48 m in width and with a height of 3.30 m consists of eight different cross-sections with three different dredged materials, different geosynthetics solutions, and varying slope inclination. It consists of two parallel dikes (with total length of embankment crown of about 260 m), one for seepage (East) and one for overflowing experiments (West), which can be performed by filling the polders with water (Cantré et al., 2013).

3. Data Acquisition

3.1 Applied Sensors

Two different sensor systems are applied to acquire data for the processing of DSMs. First, the MD4-1000, a quadrocopter from Microdrones with a digital camera from Olympus (PEN e-P2) and a fixed focal length lens of 17 mm and secondly, the AscTec Falcon 8, an octocopter from Ascending Technologies with the digital camera Sony NEX-5 and fixed focal length lens of 16 mm. Both Mini-UAVs are equipped with a consumer grade digital camera.

The UAS are standard models without further additions and integrates GPS (Global Positioning System), IMU (Inertial Measurement Unit) and an active stabilizing camera mounts compensated nick and roll vibrations.

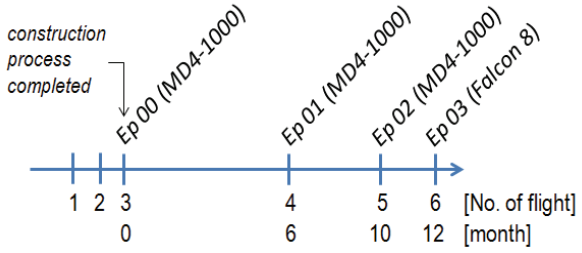

Fig 2. UAS campaigns and DSM epochs

For georeferencing and accuracy assessments of the UAS photogrammetry derived data the position of control points (Ground Control and Check Points) were determined by Real Time Kinematic (RTK) GPS in reference to virtual reference stations (VRS) calculated from SAPOS-HEPS (High Precision Realtime Positioning Service) with a standard deviation of few centimeters.

Furthermore, periodically observed subsidence control points were surveyed by a tacheometer (Leica TCRP 1207) in respect to the dike survey benchmark network with standard deviation of 1 to 2 cm. These tacheometer-determined points act as UAS-independent check points for the quality check of the UAS DSMs of epochs 00, 02 and 03.

3.2 Field Campaigns

In 2012, the area was surveyed by UAS photogrammetry four times: twice during the construction process of the dike (3th of May in 2012 and 23th of May in 2012) and twice after finishing the construction (11th of June in 2012 and 12th of December in 2012). In 2013, two more UAS surveys were conducted (16th of April in 2013 and 17th of June in 2013).

In our investigations for all subsequent measurements, flight number 3 is taken as the reference epoch (called Epoch 00) for the subsidence analysis.

3.3 Image operational flights

An UAS built-in autopilot relies on a set of rate gyroscopes, accelerometers, pressure sensors and a GPS to compute and control the state of the UAS and to follow a 3D path defined by waypoints (Küng et al., 2012).

For the autonomous image acquisition managed by the autopilot a flight planning is necessary. The camera parameters (focal length and sensor size), the desired ground resolution and the object heights define the altitude above ground. In order to support the automatic processing by a stable image block very high image overlaps are needed.

An essential prerequisite for UAS photogrammetry is the automated detection of tie points in the heterogeneous surface texture. The flying height and sufficiently bright but diffuse lighting conditions are also important.

In the area overshadowing objects (trees, etc.) are not present, so that it can be covered with nadir images.

Tab 1. Sensors and parameters of the used operational flights

No. flight	3	4	5	6
No. epoch	Ep 00	Ep 01	Ep 02	Ep 03
Date of flight	11th of June in 2012	12th of December in 2012	16th of April in 2013	17th of June in 2013
Platform and sensor				
UAS	MD4-1000	MD4-1000	MD4-1000	Falcon 8
Camera	Olympus PEN e-P2	Olympus PEN e-P2	Olympus PEN e-P2	Sony NEX-5
Focal [mm]	17	17	17	16
Sensor size [px]	3024 x 4032	3024 x 4032	3024 x 4032	3056 x 4592
Camera settings				
F-number	5.6	3.5	5.6	8
ISO-sensitivity	100	200	200	200
Exposure time	1/800	1/1000	1/1600	1/640
Flight mission				
Target of mission	Dike and nearby surrounding	Dike and extended surrounding	Dike and nearby surrounding	Dike and immediate surrounding
Covered area [ha]	3.19	5.78	2.56	1.45
Number of strips	5	5	8	5
Number of images	86	124	361	80
Altitude above ground [m]	74.6	77.7	52.8	37.8
Ground sampling distance [cm]	2.55	2.45	1.47	1.31

The flying height was around 75 to 80 m above ground (flight number 3 and 4). 5 flight strips are necessary to cover the dike and adjacent terrain. At predefined time intervals along flight path the camera was triggered, so that at the flight campaigns 86 and 124 images were recorded.

In all flights high along overlaps of about 80 % and side lap of more than 60 % could be achieved. Each surface element of the dike is redundantly represented in a lot of pictures (mostly between 4 and 9 images). These results in a ground sampling distance (GSD) of about 2.5 cm per pixel (Flight number 3 and 4).

The following investigations should focus on the dike itself. Therefore, the flight planning was modified. In flight 5, we also used the MD4-1000. However, in addition to the covered area the number of strips was increased to 8 and the altitude was reduced of about 53 m above ground which corresponds to a GSD of about 1.5 cm.

For the flight number 6, the octocopter AscTec Falcon 8 was used together with Sony NEX-5(16 mm fixed focal) at an altitude of about 45 m, these results in a ground resolution of about 0.015 m. The flight was carried out in 5 strips, while 80 images were triggered at predefined positions for imaging the dike and its immediate surrounding area.

For the flights, the aperture and shutter times were manually preset to the cameras, the latter to avoid motion blur depending on the lighting situation to values between 1/1600 and 1/640 seconds.

Tab 2. Accuracy and numbers of RTK-measured GCPs.

No. flight No. epoch	3 Ep 00	4 Ep 01	5 Ep 02	6 Ep 03
StdDev of GCP/CP in Easting, Northing, Height by Leica LGO [m]	0.007, 0.004, 0.013	0.014, 0.010, 0.027	0.012, 0.007, 0.026	0.011, 0.005, 0.015
No. of GCP	11	10	19	6
No. of CP	9	6	0	16

The texturing of the surface changed during the periods. For epoch 0 no or little vegetation was present just before sowing, but in some areas quickly productive species weed and traces of manufacturing, (e.g. vehicle tracks) were clearly visible. In the first epoch the surface was in some areas overgrown with weeds which had reached about 3-4 times the height of the grass. In epoch 02 and 03 the grass cover were closed in most places and were mowed in many parts a few weeks before flight.

4. Automated Data Processing

4.1 Processing workflow

For data processing of the imagery, state-of-the-art web processing service (WPS) using Pix4UAV Cloud were used to compute the photogrammetric products: 3D point cloud, DSM and ortho photo mosaic.

The WPS Pix4UAV Cloud offers an easy-to-use widely automated processing service with a fee model which is based on demand and size of area (Pix4D, 2014). Relatively small data preparations are necessary.

In the Pix4UAV client software, the image coordinates for the GCPs were manually measured and linked to corresponding ground coordinates. The approximated image positions based on the GPS measurements of the autopilot are also needed as input data. In preparation for the fully automatic calculation no more manual work is necessary. The software performs the following steps (Strecha et al., 2012, Küng et al., 2012):

- Searching for matching points by analyzing all images using an improved version of the binary descriptors for SIFT (Scale-invariant feature transform) method.
- Reconstruction of the exact position and orientation of the camera for every acquired image based on these matching points and approximations of the image position provided by the UAS autopilot. Initial values for the image orientations are no longer needed in current software versions. GCPs with corresponding imported image points can be included in this bundle block adjustment (Eltner et al., 2013).
- Verifying the matching points and calculation of their 3D coordinates in the coordinate reference system WGS84 using the on-board UAS GPS measurements.
- Interpolation of these points to a triangulated irregular network (TIN) and densification into a dense DSM.
- Calculation of the geo-referenced ortho photo mosaic by projecting each pixel on the DSM.

4.2 Camera calibration

Both applied cameras are non-metrical amateur systems. Compact cameras are known as sensitive to temperature differences, changes of air pressure, vibrations and shocks (Pix4D, 2013). A complete camera calibration is necessary for each flight. The self-calibration (lens distortions, focal length, principal point position) and the corrections of the images are part of the WPS.

Of course, undistorted images could be used and in some cases it has advantages, however, so that a further preparation step of the user is required. Eltner et al., 2013 reported some disadvantages in case of distorted images of the camera Panasonic Lumix, which showed in one test site in DSM processing 12 % less points are achievable with the undistorted images.

In our evaluations, we were aimed at a high degree of automation and therefore the potential of pre-calibrated undistorted images has not been studied.

4.3 Ground Control Points (GCP)

GCPs are not strictly necessary in Pix4UAV, but for a more accurate georeferencing of the photogrammetric products these are indispensable (Strecha et al., 2012) Furthermore, Ruiz et al., 2013 emphasize the necessity of GCPs as significant opportunity for improvement in spatial accuracy. They were included, together with corresponding image points, within the bundle block adjustment in Pix4UAV.

In each campaign coded marks were arranged temporary on and around the dike, they acted as GCPs or control points (CP) for verifications about the accuracy (cross validation). Their 3D positions were determined by means of RTK-GPS using the reference signals of SAPOS-HEPS (Satellite Positioning Service – High Precise Realtime Positioning Service) with standard deviations in range of few centimeters, calculated through Leica GeoOffice 8.1 (Tab 2).

4.4 Assessment of DSM accuracy

4.4.1 Overall accuracy of the DSM based on the dike surface mainly without vegetations (epoch 00)

The flight number 3 (epoch 00) was used for a detailed comparison of accuracy against the Terrestrial Laser Scanning (TLS). The investigation showed that the UAS DSM for the dike surface mainly without vegetations has a high level of agreement in the majority of

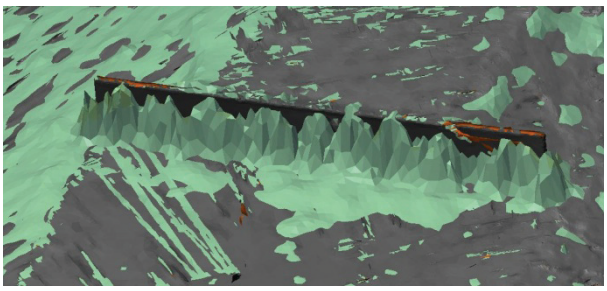

Fig 3. Overlay of UAS-DSM epoch 00 (green) and TLS-DSM (gray)

areas (gradual curvature change) with a standard deviation of about 2.2 - 4.0 cm (filtered vs unfiltered) compared to the TLS model. This comparison included 681338 points (Naumann et al., 2013).

Problematic locations for the UAS photogrammetry with nadir-looking cameras are areas, which are not very well textured, are too small or have abrupt jumps in height, e.g. retaining wall and their faces built up as limits of the flooding areas (Fig. 3). For those partial areas in our study site the accuracy is slightly worse (errors in the range of one to two decimeters). In further studies on the deformations, we therefore removed the areas of retaining wall from the DSMs.

An additional verification based onto independent tacheometrically measured control points confirmed this consensus. At 34 points, distributed over the dike, the standard deviation of all the height differences is 0.028 m.

4.4.2 Verifications of the DSMs of the following epochs

The heights of the DSMs were compared at selected points, marked on the dike by poles, with heights determined by tacheometry and temporarily markers determined in the RTK session, but which were not used for georeferencing (Tab 3).

On the RTK control points, the mean deviation is nearly zero (except epoch 01) and the standard deviations are mainly in the expected range.

The mean deviations on the tacheometer control points show a systematic shift (UAS above Tacheometer), due to the growth of vegetations at these locations and the standard deviation is in a range of 2 to 3 cm.

The verification of the DSM of epoch 01 shows on the RTK control points a significant increased standard deviation. The standard deviation of four checkpoints in the western part of the polder 1 and on the eastern border of the polder is in the range between -0.269 m and +0.143 m. For further analysis, unfortunately there are no heights of tacheometry available for this period. For this epoch greening in most areas had attained the highest vegetation height of all surveyed epochs. Following the last mowing, about two months ago, especially the dicotyledonous weeds grew at about 3-4 times the height of the grass. In conjunction with the seasonal low sun long shadows appeared it showed in some areas less favorable contrast ratios, which led to inaccurate surface calculations probably due to incorrect matching on thin plant structures.

The reason could also be an incorrect measurements of GCPs in the images, because on this flight smaller markers were used, which are more suitable for the lower altitudes above ground flown in epoch 02 and 03. To evaluate this, more experiments are necessary.

For subsequent epochs, the flying altitude was reduced, which improves the image resolution and search for matching points in the images by increasing the textural differences within the vegetation areas.

5. Multi-temporal change detections using UAS Photogrammetry

For some research topics, such as subsidence, consolidation and increased surface erosion, the comparison of high-resolution DSM of different times (change detection) is appropriate. Such evaluations can also serve for the control of the production process, e.g. for verification of material thickness during construction.

The settlements of the dike were expected in the range of tens of centimeters. The geotechnical monitoring program with a variety of built-in sensors, takes into account that temporal changes in height of the dike surface are caused not only by consolidations of the materials but also through subsidence of the subsurface.

5.1 Processing of difference models

In a preprocessing the areas with heavy vegetation growth (south slope of polder 1), abrupt jumps in height (sheet pile wall) or man-made obstructions on the dike surface (e.g. persons, technical equipment, installations) were eliminated in all DSMs (in the figure showing the differences between epochs recognizable as masked white areas). All operations, masking, calculations of the height differences between the DSMs and their map representations were performed with ESRI ArcGIS. We

Tab 3. Accuracy assessment of the DSMs

No. flight No. epoch	3 Ep 00	4 Ep 01	5 Ep 02	6 Ep 3
DSM vs. RTK-Check Points: Mean and StdDev of differences in heights [m] (No. of Samples)	0.005 ± 0.013 (9)	-0.040 ± 0.130 (6)	-0.003 ± 0.019 (determined on the 19 GCPs)	0.001 ± 0.010 (16)
DSM vs. Tacheometer-Check Points: Mean and StdDev of differences in heights [m] (No. of Samples)	0.027 ± 0.028 (34)	--- (no survey in this period)	0.032 ± 0.024 (41)	0.041 ± 0.018 (32)
DSM vs TLS-DSM: StdDev of differences in heights [m]	0.040 (0.022 with filtering deviations >10 cm)	---	---	---

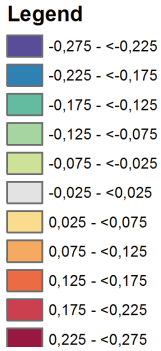

Fig 4. Color classification used for the height differences

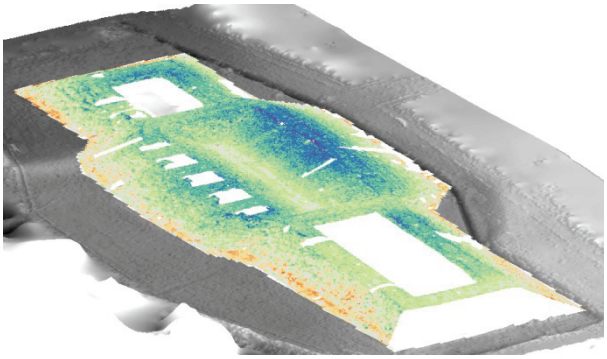

Fig 5. Difference model Ep03-Ep00 draped on DSM Ep 03

calculated differences along the z-axis (height) to the epoch 00 as well as differences between successive epochs.

For the accuracy analysis in this paper we use the class formation and color gradations according to Fig. 4. The differences were classified in steps of 5 cm. Increases are shown in color shades of ocher to red and decreases from light green to purple (Fig. 5). The neutral color class in gray with values between -2.5 cm and 2.5 cm represents the noise of the measurement method, as it was determined in Naumann et al., 2013.

5.2 Changes with respect to epoch 00

As a result of our evaluation, we were able to detect the most striking areas of subsidence in every epoch (Ep01-Ep00, Ep02–Ep00, Ep03-Ep00) in the eastern upper slope area of the second polder (Fig. 6).

Areas with positive height difference are mainly due to vegetation growth. The average height of the grass varied between epochs and in smaller areas also even within an epoch. This is problematic for the UAS photogrammetry and sometimes leads to misinterpretation, because areas with positive height difference may mainly be explained by vegetation growth, but also alleged subsidence can be caused by a decline in plant height. This can be seen in our case, if an epoch shows values against the trend.

For instance, the surface differences in southern inner slope area shows an increase of the surface in epoch 02 (high plant height), but a decrease in epoch 03 (low plant height).

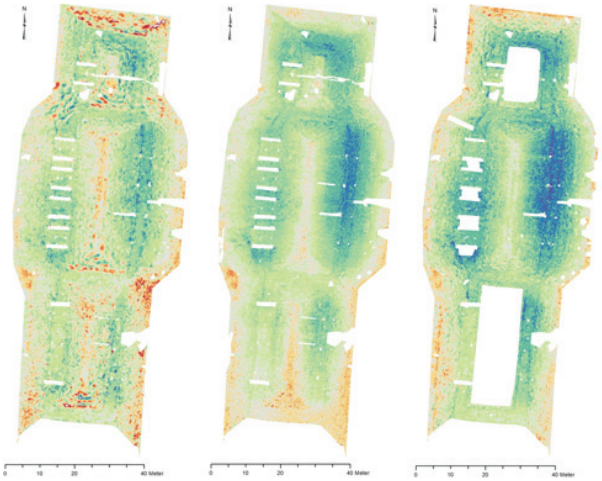

Fig 6. Differences in dike surfaces after 6, 10 and 12 months (Ep01-Ep00, Ep02-Ep00, Ep03-Ep00)

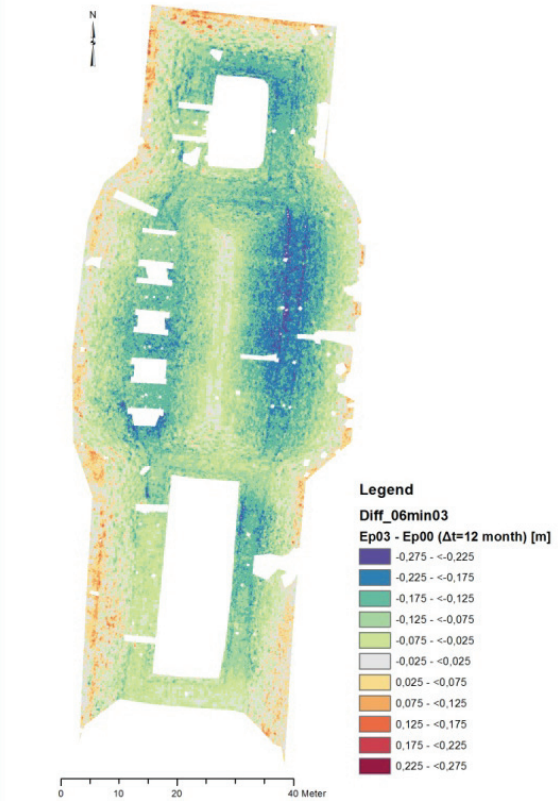

Fig 7. Differences in heights between dike surfaces after 12 months (Ep 03 minus Ep 00)

Conversely, larger subsidence exhibits the comparison of epoch 01 to epoch 00, which is not confirmed in the subsequent period, due to the partially as incorrect detected epoch 01 (mainly in south-western embankment).

The volume and therefore the weight of the eastern dike are greater than those of the western dike. Therefore, the stronger surface reductions result probably due to increased subsidence of subsurface. After 12 months, these were predominantly in the range from 17.5 to 22.5 cm (Fig. 7).

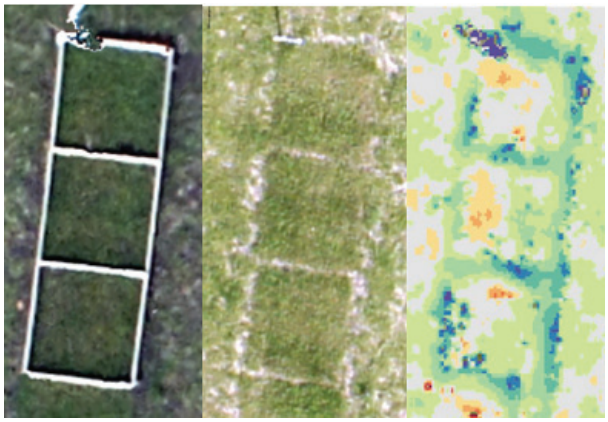

Fig 8. Removal of a small boundary wall of a study area for planting (images of Ep 02, Ep 03 and difference model)

5.3 Changes between successive epochs

In contrast, the course of the consolidation of settlements can be better analyzed by comparisons of sequential epochs (Ep01-Ep00, Ep02-Ep01, Ep03-Ep02).

The differentiability of objects on the surface could be improved significantly during the experimental campaigns only within the image data, due to the higher resolution at lower altitude and the higher number of images that represent an object. In contrast, the detailing of the surface models did not improve in the same scale, due to the increase of vegetation density. It can be stated that the adjustment of flight parameters ensured the accuracy of the DSM even in vegetation growth.

So smaller man-made changes could successfully be detected, for instance a demarcated sample grid (height of wall about 12 cm) was dismantled between epoch 02 and epoch 03 (Fig. 8).

5.3 Independent control of temporal height changes

Due to the selective review of individual surface models with RTK or tacheometry the accuracies of the differences are also in the range of a few centimeters.

Exceptions are the difference models, where epoch 01 is involved, due to the already discussed faults in the DSM of epoch 01. Changes shown in the southwest embankment are proved by the subsequent era as faulty (one to two decimeters).

6. Conclusions

Micro-UAS are easy to use, handle complex predefined trajectories, capture images at predefined points, attain very high image overlaps, reduce the time required for site survey greatly and thus allow (under regulation of the weather conditions and the battery reserves) repeated measurements of the entire area within short periods.

Nevertheless, the accuracy of an automatically calculated UAS DSM depends on a variety of parameters that can be assigned to the following domains:

- camera and flight: ground resolution, image overlap, number of rays from different images to the very same point, stable interior orientation of the camera,
- property and lighting of the object: density and height of vegetation, texturing, sufficiently bright but diffuse lighting, if possible no shading and continuous surface shape,
- GCPs: accuracy, recognizability and distribution of the points.

High accuracy in the determination of deformations between DSMs of various epochs can only be achieved when uniform growth conditions are ensured. If possible, before each UAS surveying the dike should be mowed or same growth stages should predominate.

The accuracy verification of the DSM showed standard deviations of the height differences between 2 and 3 cm. Subsidence about 2 to 3 times larger than the standard deviation can be clearly detected. The UAS photogrammetry is suitable to detect the changes between DSMs of dike construction works area-wide, if their magnitudes are above the measurement uncertainty and the change of vegetation heights between epochs. The results are transferable to other objects with continuous surface shape and without sudden jumps of the heights. At such edges or thin obstructions increased errors can be reported.

In addition, the accuracy can be achieved by modifications of the flight, for example, by increasing the resolution by reducing the altitude, adaptation of the flight trajectory to difficult areas of the object (pattern instead of strips), increasing the detection accuracy of specific objects such as vertical walls by additional oblique looking camera shots.

The accuracy assessment could be improved by using check points without signaling by neighboring rods or poles. Instead of check points marked reference areas, for instance suitable textured plates could be implemented on the surface. Their orientations are to be determined by a number of points (e.g. tacheometry). These reference surfaces can be compared with the corresponding regions of the DSM.

Nomenclature

AdV: Working Committee of the Surveying Authorities of the States of the Federal Republic of Germany
Ep: Epoch
CP: Control Point
DSM: Digital Surface Model
GCP: Ground Control Points
GPS: Global Positioning System (USA)
IMU: Inertial Measurement Unit
LGO: Leica GeoOffice
RTK: Real Time Kinematic GPS
RPAS: Remotely piloted aircraft systems
SAPOS®: Satellite Positioning Service (AdV, Germany)
StdDev: Standard Deviation
TLS: Terrestrial Laser Scanning
TIN: Triangulated Irregular Network

UAS: Unmanned Aerial Systems
UAV: Unmanned Aerial Vehicle

References

Cantré, S.; Große, A.-K.; Neumann, R.; Nitschke, M.; Henneberg, M.; Saathoff, F., 2013. *Fine-grained organic dredged materials for dike cover layers – Material characterization and experimental results*. WODCON XX 2013, Brussels, Belgium, Proceedings, URL: http://www.dredgdikes.eu/ (03.01.2014).

Cantré, S., Saathoff, F., 2013. *Installation of fine-grained organic dredged materials in combination with geosynthetics in the German DredgDikes research dike facility*, Engineering Structures and Technologies, 5:3, 93-102.

Eisenbeiss, H., 2009. *UAV Photogrammetry*. Ph.D. thesis, Zürich: Institute of Geodesy and Photogrammetry, ETH Zurich, Switzerland, Mitteilungen Nr.105, 235 p.

Eisenbeiss, H., Zhang, L., 2006. *Comparison of DSMs generated from mini UAV imagery and terrestrial laser scanner in a cultural heritage application*. ISPRS (International Archives of Photogrammetry, Remote Sensing and Spatial Information Sciences), Commission V Symposium, Image Engineering and Vision Metrology, Dresden, Germany, 25.-27. September 2006, In: ISPRS, Vol. XXXVI-Part5, pp. 90-96.

Eltner, A.; Mulsow, C.; Maas, H.-G., 2013. *Quantitative Measurement of soil erosion from TLS and UAV data*. International Archives of Photogrammetry, Remote Sensing and Spatial Information Sciences, Vol. XL-1/W2, pp. 119-124.

González-Aguilera, D.; Fernández-Hernández, J.; Mancera-Taboada, J.; Rodríguez-Gonzálvez, P.; Hernández-López, D., Felipe-García, B.; Gozalo-Sanz, I.; Arias-Perez, B., 2012. *3D Modelling and accuracy assessment of granite quarry using unmannend aerial vehicle*. ISPRS (International Archives of Photogrammetry, Remote Sensing and Spatial Information Sciences) Commission V Symposium, Image Engineering and Vision Metrology, Melbourne, Australia, In: ISPRS Vol. XXII, pp. 37-42.

Küng, O.; Strecha, C.; Beyerler, A.; Zufferey, J.-C; Floreano, D.; Fua, P.; Gervaix, F., 2012. *The accuracy of automatic photogrammetrie techniques on ultra-light UAV imagery*. ISPRS (International Archives of the Photogrammetry, Remote Sensing and Spatial Information Sciences), Vol. XXXVIII-1, Part C22

Naumann, M.; Geist, M.; Bill, R.; Niemeyer, F.; Grenzdörffer, G., 2013. *Accuracy comparison of Digital Surface Models created by Unmanned Aerial Systems imagery and Terrestrial Laser Scanner*. ISPRS (International Archives of the Photogrammetry, Remote Sensing and Spatial Information Sciences), UAV-g2013, 4.-6. September 2013, Rostock, Germany, In: ISPRS, Commission IVWG I/5, Volume XL-1/W2, 2013.

Pix4D, 2014. *Product overview* (website), URL: http://www.pix4d.com/ products/ (10.01.2014).

Pix4D, 2013. Knowledge Base, FAQ, Feature description (website), URL: https://support.pix4d.com/entries/ 36814253-Features-description (10.01.2014).

Ruiz, J.J.; Diaz-Mas, L.; Perez, F.; Viguria, A. 2013. *Evaluating the accuracy of DEM generation algorithms from UAV imagery*. ISPRS (International Archives of the Photogrammetry, Remote Sensing and Spatial Information Sciences), UAV-g2013, 4 – 6 September 2013, Rostock, Germany, In: ISPRS, Commission IVWG I/5, Volume XL-1/W2.

Sauerbier, M.; Siegrist, H.; Eisenbeiss, H.; Derrir, N., 2011. *The practical application of UAV-based Photogrammetry under economic aspects*. International Archives of Photogrammetry, Remote Sensing and Spatial Information Sciences, UAV-g 2011, Conference on Unmanned Aerial Vehicle in Geomatics, Zurich, Switzerland, In: ISPRS Vol. XXXVIII-1/C22.

Strecha, C.; Küng, O.; Fua, P., 2012. *Automatic mapping from ultra-light UAV imagery*. EuroCOW 2012, Barceloa, Spain, 8.-10. February, 2012. URL: http://infoscience.epfl.ch/record/175351/files/eurocow_strecha.pdf (12.01.14).